Accepted Manuscript

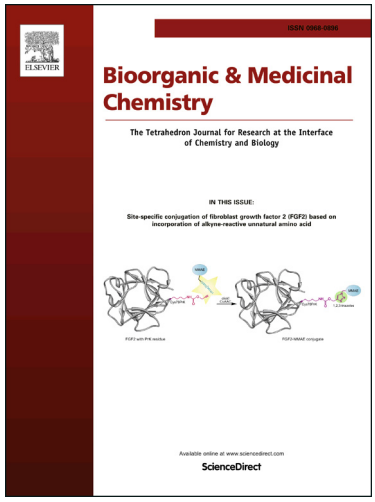

Design, synthesis and biological evaluation of novel hydroxamic acid based histone deacetylase 6 selective inhibitors bearing phenylpyrazol scaffold as surface recognition motif

Jinyu Yang, Gaoliang Cheng, Qihao Xu, Shenglin Luan, Shuxiang Wang, Dan Liu, Linxiang Zhao

PII: S0968-0896(17)31490-6
DOI: http://dx.doi.org/10.1016/j.bmc.2017.08.029
Reference: BMC 13932

To appear in: *Bioorganic & Medicinal Chemistry*

Received Date: 20 July 2017
Revised Date: 15 August 2017
Accepted Date: 17 August 2017

Please cite this article as: Yang, J., Cheng, G., Xu, Q., Luan, S., Wang, S., Liu, D., Zhao, L., Design, synthesis and biological evaluation of novel hydroxamic acid based histone deacetylase 6 selective inhibitors bearing phenylpyrazol scaffold as surface recognition motif, *Bioorganic & Medicinal Chemistry* (2017), doi: http://dx.doi.org/10.1016/j.bmc.2017.08.029

Design, synthesis and biological evaluation of novel hydroxamic acid based histone deacetylase 6 selective inhibitors bearing phenylpyrazol scaffold as surface recognition motif

Jinyu Yang, Gaoliang Cheng, Qihao Xu, Shenglin Luan, Shuxiang Wang, Dan Liu*, Linxiang Zhao*

Key Laboratory of Structure-Based Drugs Design & Discovery of Ministry of Education, Shenyang Pharmaceutical University, Shenyang 110016, China

*Corresponding authors.

Tel./Fax: +86 024 4352 0221.

E-mail address: sammyld@163.com (D. Liu);

linxiang.zhao@vip.sina.com (L. Zhao)

Abstract

In recent years, inhibition of HDAC6 became a promising therapeutic strategy for the treatment of cancer and HDAC6 inhibitors were considered to be potent anti-cancer agents. In this work, celecoxib showed moderate degree of HDAC6 inhibition activity and selectivity in preliminary enzyme inhibition activity assay. A series of hydroxamic acid derivatives bearing phenylpyrazol moiety were designed and synthesized as HDAC6 inhibitors. Most compounds showed potent HDAC6 inhibition activity. **11i** was the most selective compound against HDAC6 with IC_{50} values of 0.020 μM and selective factor of 101.1. Structure-activity relationship analysis indicated that locating the linker group at 1' of pyrazol gave the most selectivity. The most compounds **11i** (GI_{50} = 3.63 μM) exhibited 6-fold more potent than vorinostat in HepG2 cells. Considering of the high selectivity against HDAC6 and anti-proliferation activity, such compounds have potential to be developed as anti-cancer agents.

Keywords: Phenylpyrazole derivatives; HDAC6 selective inhibitor; Anti-proliferative activity; Structure-activity relatonship.

1. Introduction

The acetylation level of histone regulated by histone acetyl transferases (HATs) and histone deacetylases (HDACs) plays an important role in the development of many diseases such as HIV, HCV, cancer *etc.*[1, 2]. The 18 isoforms of HDACs are grouped into four classes: class I (HDACs 1, 2, 3 and 8), class II (HDACs 4, 5, 6, 7, 9 and 10), class III(SIRT1-7) and class IV (HDAC 11). The HDACs can be classified into two categories based on their mechanisms: zinc-dependent deacetylases (class I, II and IV) and class III NAD^+-dependent (class III) deacetylases [3]. Inhibition of HDACs has been proved to be an effective therapeutic strategy for cancers[4]. There are five agents have been approved by FDA or CFDA (Vorinostat[5], Romidepsin[6], Panobinostat[7], Belinostat[8] and Chidamide[9]) for the treatment of lymphoma and multiple myeloma. However, all the approved drugs are class I selective or pan-HDAC inhibitors which have multiple side-effects as reported[10].

HDAC6, which is primarily located at cytoplasm, deacetylated lysine residues of many non-histone substrates, including Hsp90, α-tubulin and Ku70[11, 12]. Recently, The dysregulated expression of HDAC6 was proved to be related to many diseases exemplified by HIV[13], Alzheimer's disease[14], inflammation[15] and cancer[16]. Development of HDAC6 selective inhibitors as novel anticancer agents seemed to be preferable than the pan-inhibitors, considering the fact that HDAC6 selective inhibitors showed fewer side-effects[17]. To date, Tubacin[18], ACY-1215[19], tubastatin A[20] and other HDAC6 selective inhibitors have been reported by many groups. Among them, ACY-1215 is the most promising molecule of which phase II clinical trial for treating multiple myeloma has been completed. All these achievements prompted us to develop potent HDAC6 inhibitors with high selectivity. Considering all the reported structures, a HDAC6 inhibitor can be divided into three pharmacophores: (1) zinc-binding group (ZBG), interacting with the Zn^{2+} at the bottom of the active site; (2) linker group, matching the hydrophobic tunnel of HDAC6; (3) surface recognition motif (SRM), covering the entrance of the active pocket.

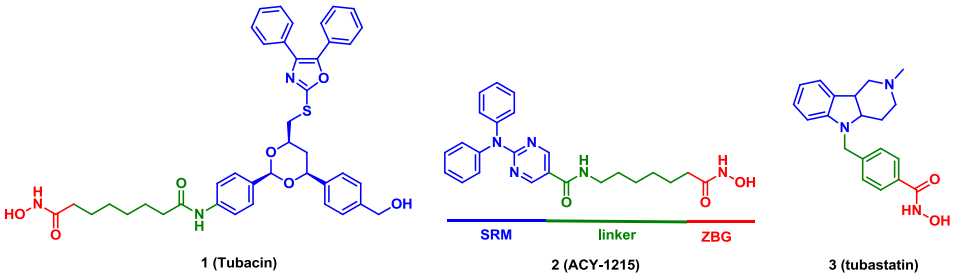

Figure 1. Structures of some reported HDAC6 inhibitors

In our previous study, a small library of approved drugs was screened for inhibitory activity of HDAC6 using fluorescence assay. Celecoxib, an anti-inflammatory drug, which is also accounted as a carbonic anhydrase II inhibitor for its zinc binding capacity[21], showed moderate degree of HDAC6 inhibition and selectivity (IC_{50} = 0.643 μM and SF = 1.8). In addition, celecoxib was well tolerated and had no clinically significant adverse effects with the total daily dosage of 400 mg in a six weeks trial[22]. Considering the activity, selectivity and security, we chose celecoxib as an outstanding lead compound for the development of HDAC6 selective inhibitors in this study. We designed and synthesized a series of phenylpyrazole derivatives based on celecoxib. Several modifications of celecoxib were performed to improve the potency and selectivity: (1) to increase HDAC6 binding affinity, the sulfanilamide group was replaced by hydroxamic acid in order to chelate Zn^{2+} by more coordination bond; (2) based on the conception that SRM structures strongly influence the selectivity of compounds against HDAC isotype[23], a SAR study for the SRM by changing the location of linker group on pyrazole was proceed to optimize HDAC6 selectivity of the lead compound; (3) to deeply discuss the effect of linker group on the activity and selectivity against HDAC6, the phenyl was replaced by several linear alkyls of different lengths.

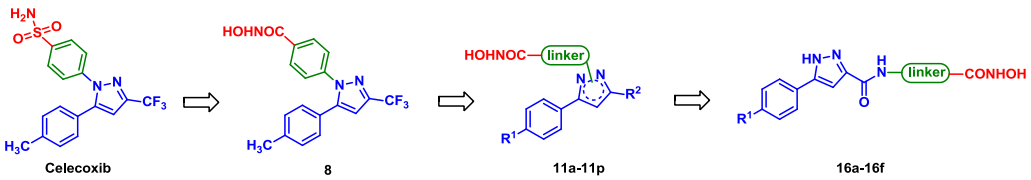

Figure 2. Rational design of Celecoxib derivatives

2. Results and discussion

2.1. Chemistry

The synthetic route to compound **8** was illustrated as **Scheme 1**. A condensation reaction of *p*-methylacetophenone **5a** with trifluoroacetic acid ethyl ester in THF at room temperature was performed to obtain dione **6a,** which was coupled with sulfonamidophenylhydrazine hydrochloride in the next step. Intermediate **7** was reacted with 50% hydroxylamine to afford the designed hydroxamic acid **8**.

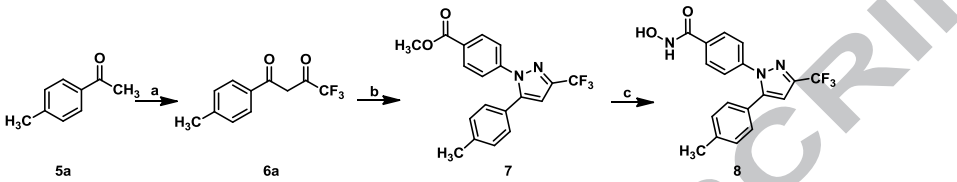

Scheme 1. Synthesis of target compound **8**. Reagents and conditions: (a) Ethyl trifluoroacetate, NaOMe, THF, reflux, 5h; (b) Methyl 4-hydrazinylbenzoate, EtOH, reflux, 4h; (c) 50% NH_2OH, NaOH, MeOH, r.t., 3h.

Compounds **11a-11p** were synthesized from substituted acetophenones **5a-5c** by the route displayed in **Scheme 2**. Compounds **6a-6g** were treated with hydrazine hydrate in acetic acid at 120°C to give intermediates **9a-9g**. Intermediates **9a-9g** were reacted with methyl 4-(bromomethyl)benzoate or methyl 4-(2-bromoethyl)benzoate, then the ester groups of products were converted into the corresponding hydroxamic acids of **11a-11p**.

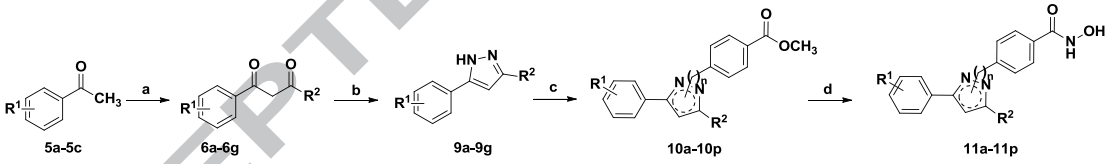

5a R^1 = Me
5b R^1 = -CH_2OCH_2-
5c R^1 = F

6a R^1 = Me, R^2 = CF_3
6b R^1 = Me, R^2 = Me
6c R^1 = -CH_2OCH_2-, R^2 = Me
6d R^1 = F, R^2 = Me
6e R^1 = F, R^2 = Et
6f R^1 = F, R^2 = n-propyl
6g R^1 = F, R^2 = benzyl

9a R^1 = Me, R^2 = CF_3
9b R^1 = Me, R^2 = Me
9c R^1 = -CH_2OCH_2-, R^2 = Me
9d R^1 = F, R^2 = Me
9e R^1 = F, R^2 = Et
9f R^1 = F, R^2 = n-propyl
9g R^1 = F, R^2 = benzyl

10a, 10b R^1 = Me, R^2 = CF_3, n = 1
10c, 10d R^1 = Me, R^2 = CF_3, n = 2
10e, 10f R^1 = Me, R^2 = Me, n = 1
10g, 10h R^1 = -CH_2OCH_2-, R^2 = Me, n = 1
10i, 10j R^1 = F, R^2 = Me, n = 1
10k, 10l R^1 = F, R^2 = Et, n = 1
10m, 10n R^1 = F, R^2 = n-propyl, n = 1
10o, 10p R^1 = F, R^2 = benzyl, n = 1

11a, 11b R^1 = Me, R^2 = CF_3, n = 1
11c, 11d R^1 = Me, R^2 = CF_3, n = 2
11e, 11f R^1 = Me, R^2 = Me, n = 1
11g, 11h R^1 = -CH_2OCH_2-, R^2 = Me, n = 1
11i, 11j R^1 = F, R^2 = Me, n = 1
11k, 11l R^1 = F, R^2 = Et, n = 1
11m, 11n R^1 = F, R^2 = n-propyl, n = 1
11o, 11p R^1 = F, R^2 = benzyl, n = 1

Scheme 2. Synthesis of target compounds **11a-11p**. Reagents and conditions: (a) Substituted carboxylic ethyl ether, NaH, anhydrous THF, N_2, r.t., overnight; (b) hydrazine hydrate, acetic acid, reflux, 2h; (c) methyl 4-bromomethyl benzoate or methyl 4-(2-bromoethyl)benzoate, K_2CO_3, MeCN, reflux, 4h; (d) 50% NH_2OH, NaOH, MeOH, r.t., 3h.

The synthetic route to compounds **16a-16f** was depicted in **Scheme 3**. Intermediate **14** was synthesized from 4-fluoroacetophenone through condensation, cyclization and hydrolysis successively. Intermediate **14** was coupled with appropriate amino acid methyl esters to afford the required amides **15a-15f**, which were treated with 50%

hydroxylamine to produce **16a-16f**.

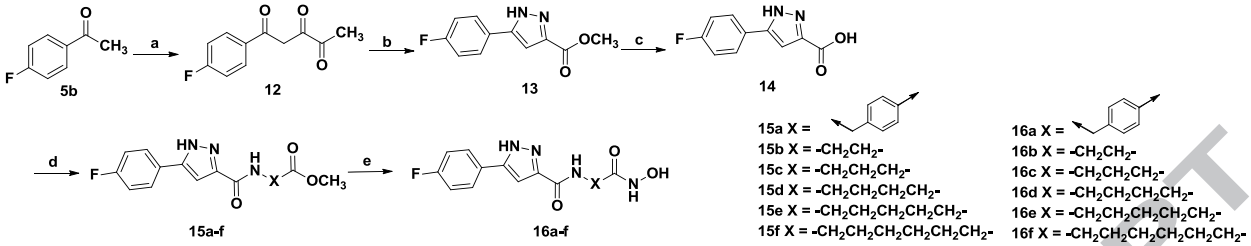

Scheme 3. Synthesis of target compounds **16a-16f**. Reagents and conditions: (a) Dimethyl oxalate, NaOMe, diethyl ether, r.t., overnight; (b) hydrazine hydrate, acetic acid, reflux, 2h; (c) NaOH, H_2O, reflux, 2h; (d) appropriate amino acid methyl esters, HOBt, EDCI, TEA, DMF, r.t., overnight; (e) 50% NH_2OH, NaOH, MeOH, r.t., 3h.

2.2 *In vitro* HDAC inhibition and selectivity

The HDAC inhibition activities of novel compounds against HeLa nuclear extracts and recombinant human HDAC1, 2, 3, 6, 8 enzymes were investigated, using vorinostat and Rolinostat as positive controls. As shown in **Table 1** and **Table 2**, the ZBG motif had a significant influence on HDAC inhibition activity. Compound **8** (IC_{50}= 0.359 μM) with a hydroxamic acid group showed more potent activity against HDAC6 than celecoxib (IC_{50}= 0.643 μM). The substituent groups on benzene ring of SRM also have influence on the selectivity. When the linker is on 1' of the pyrazol, the activity against HDAC6 follows the trends of **11e** (R^1 = Me, IC_{50} = 0.029 μM), **11g** (R^1 = 3, 4-OCH_2O, IC_{50} = 0.036 μM) and **11i** (R^1 = F, IC_{50} = 0.020 μM), suggesting a bulk substituent is unfavorable for HDAC6 inhibition activity. For the R^2 group, the selectivity and activities decreased when the substituent getting larger (exemplified by **11i**, **11k** and **11m**). For the distance between pyridine and the phenyl in linker, carbon length with n = 1 (**11a** and **11b**) gave the superior activities with IC_{50}s of 0.027 μM and 0.016 μM against HDAC6, respectively. Systematic evaluation reflected that the position of linker on pyrazol largely influenced HDAC6 selectivity (1' substituted > 2'- substituted > 3'- substituted). For example, compound **11i** is the most selective HDAC6 inhibitor with a SF of 101.1 which higher than **11j** (SF = 60.0) and **16a** (SF = 38.0). For the linker group, benzene ring is favorable for HDAC6 selectivity and the length with 5 or 6 carbon is favorable for HDAC inhibition activity (exemplified by **16a**, **16e** and **16f**).

Table 1. The HDAC inhibitory activities of compounds **8** and **11a-11p**.

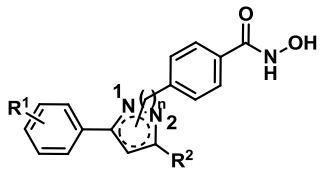

8, 11a-11p

Compd.	Linker position	R^1	R^2	n	IC_{50} (μM)						Selective factor (SF) $HDAC^{6/1}$
					HDACs	HDAC1	HDAC2	HDAC3	HDAC6	HDAC8	
Celecoxib	1	Me	CF_3	0	1.637	1.185	ND	ND	0.643	ND	1.8
8	1	Me	CF_3	0	1.139	0.836	0.919	0.736	0.359	>5	2.3
11a	1	Me	CF_3	1	0.231	0.925	1.216	0.128	0.027	>5	34.3
11b	2	Me	CF_3	1	0.033	0.110	0.047	0.021	0.016	>5	6.9
11c	1	Me	CF_3	2	1.460	1.071	0.635	0.816	0.540	>5	2.0
11d	2	Me	CF_3	2	0.121	0.352	0.549	0.080	0.078	>5	4.5
11e	1	Me	Me	1	0.022	0.694	0.076	0.053	0.029	>5	23.9
11f	2	Me	Me	1	0.013	0.133	0.041	0.026	0.007	>5	19.0
11g	1	3, 4-O CH_2O	Me	1	0.016	0.430	0.135	0.092	0.036	>5	11.9
11h	2	3, 4-O CH_2O	Me	1	0.008	0.024	0.040	0.036	0.005	>5	4.8
11i	1	F	Me	1	1.439	2.021	1.974	1.205	0.020	>5	101.1
11j	2	F	Me	1	0.040	0.480	0.114	0.069	0.008	>5	60.0
11k	1	F	Et	1	1.792	3.611	1.503	1.844	0.069	>5	52.3
11l	2	F	Et	1	0.165	0.487	0.391	0.228	0.035	>5	13.9
11m	1	F	n-propyl	1	3.827	>5	2.883	1.942	0.167	>5	
11n	2	F	n-propyl	1	0.476	0.541	0.362	0.290	0.107	>5	5.1
11o	1	F	benzyl	1	>5	>5	>5	>5	0.420	>5	
11p	2	F	benzyl	1	1.028	1.883	0.763	0.619	0.326	>5	5.8
Vorinostat					0.055	0.085	0.031	0.010	0.031	2.139	2.7
ACY-1215					ND	0.100	0.066	0.037	0.009	>5	11.1

Table 2. The HDAC inhibitory activities of compounds **16a-16f**.

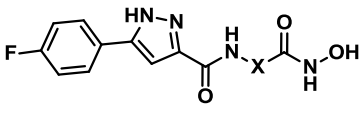

16a-16f

Compd.	X	IC_{50} (μM)						Seletivity factor HDAC6/1
		HDACs	HDAC1	HDAC2	HDAC3	HDAC6	HDAC8	
16a	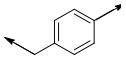	0.022	0.038	0.017	0.009	0.001	>5	38.0
16b	$-(CH_2)_2-$	>5	>5	>5	>5	>5	>5	
16c	$-(CH_2)_3-$	2.603	3.741	1.835	1.426	1.057	>5	3.5

16d	-$(CH_2)_4$-	0.644	1.039	0.883	0.671	0.275	>5	3.8
16e	-$(CH_2)_5$-	0.058	0.066	0.042	0.036	0.029	3.710	2.3
16f	-$(CH_2)_6$-	0.043	0.079	0.040	0.035	0.022	2.951	3.6
Vorinostat		0.055	0.085	0.031	0.010	0.031	2.139	2.7
Rolinostat		ND	0.100	0.066	0.037	0.009	>5	11.1

2.3 Cell growth inhibition assay

The antiproliferative effects of novel compounds were tested against A549 (human lung cancer) and HpeG2 (human liver cancer) cell lines with Vorinostat as a positive control.

The results of the anti-proliferation assay of synthesized compounds are summarized in **Table 3**. Most hydroxamate analogues manifested significant anti-proliferative activities against two tumor cell lines. Most compounds showed more potent anti-proliferation activities than vorinostat against HepG2 cells. Replacement of the methyl of **11e** (GI_{50} = 13.34 μM) by 3, 4-OCH_2O- led to decline of anti-proliferative activity (**11g**, GI_{50} = 16.48 μM). However, replacement of the methyl of **11e** by F led to increase of anti-proliferative activity (**11i**, GI_{50} = 3.63 μM). Comparison of the activities of compound **11a** (GI_{50} = 7.5 μM) and compound **11b** (GI_{50} = 8.58 μM) suggested that compounds with the linker group on 1' of the pyrazol were more potent than the corresponding 2' substituent compounds against HepG2 cell. This phenomenon could be further confirmed by **11e**, **11g**, **11i** vs. **11f**, **11h**, **11j**. These results suggesting that a small R^1 group is favorable for the inhibition activity against HepG2 cell, which is identical with the HDAC6 selectivity. For **16a-16f**, **16f** displayed the optimal activity (GI_{50} = 1.98 μM against A549 cells) suggesting the length of linker group with 6 carbon is favorable for inhibition activity. Comparison of the activities of **16a** (GI_{50} = 20.22 μM) and **16f** (GI_{50} = 1.98 μM) indicated that flexible linker group is beneficial for anti-proliferation activity.

Table 3. The anti-proliferative activities of indicated compounds and SAHA against two representative tumor cell lines

Compd.	**GI_{50} (μM)**		**Compd.**	**GI_{50} (μM)**	
	A549	**HepG2**		**A549**	**HepG2**
Vorinostat	5.02	21.96	**11j**	11.38	30.02
8	>100	>100	**11k**	16.72	7.76
11a	10.63	7.5	**11l**	19.17	16.68
11b	15.52	8.58	**11m**	16.03	6.66
11c	29.33	23.96	**11n**	15.21	16.75
11d	>100	27.58	**16a**	20.22	38.13

11e	12.38	13.34	**16b**	46.88	76.03
11f	11.16	21.18	**16c**	>100	88.01
11g	23.18	16.48	**16d**	>100	>100
11h	28.06	20.76	**16e**	7.09	47.58
11i	32.99	3.63	**16f**	1.98	23.17

2.4 Docking study

Compound **11i** was found to be an excellent HDAC6 selective inhibitor (IC_{50} = 0.020 μM and SF = 101.1) and anticancer agent (GI_{50} = 3.63 μM). The possible binding modes of **11i** on HDAC1 (PDB ID: 4BKX), HDAC 2 (PDB ID: 4LXZ), HDAC 6 (PDB ID: 5EDU) and **11g** on HDAC6 were explored using the Discovery Studio 3.0/CDOCKER protocol (**Figure 3**).

Docking studies revealed that HDAC6 contains a deeper, wider and more hydrophobic pocket formed by Phe679, Phe680, Met682, Leu749 and Gly750 than other HDAC isoforms. Analysis of the docked complexes suggested that compound **11i** could only occupy the hydrophobic pocket of HDAC6 suitably with a π–π stack between benzene ring and Phe679 for the high capacity of hydrophobic pocket (**Figure 3C**). However, **11i** showed very different conformations when binding to HDAC1 and HDAC3 (**Figure 3A, 3B**). This clear difference probably made the selectivity of **11i** against HDAC6. Notably, the hydrophobic pocket could only accommodate a benzene ring without a bulky substituent group, which explained the low selectivity of **11g** (**Figure 3D**). By analyzing the events mentioned above, we drew the conclusion that the hydrophobic pocket is a characteristic of HDAC6 and a benzene ring with a small substituent at SAM moiety is significative for HDAC6 selectivity.

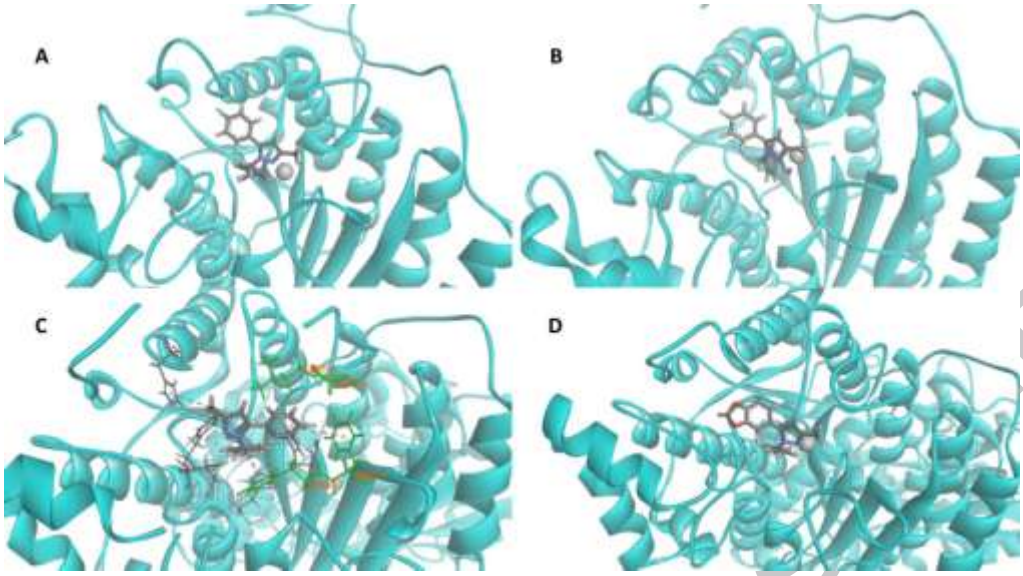

Figure 3. Possible binding modes of **11i** to HDAC1 (A), HDAC2 (B), HDAC6 (C) and **11g** to HDAC6 (D).

3. Conclusion

In our study, a series of phenylpyrazole hydroxamate analogues have been designed and synthesized. The synthesized compounds were investigated for their enzyme inhibitory activities against HDAC1, 2, 3, 6 and 8 as well as their *in vitro* antiproliferative activities against three human cancer cell lines including A549 and HepG2. Compound **11i** demonstrated the supreme HDAC6 selectivity, which was much higher than Vorinostat and Rolinostat. Compound **11i** also showed the supreme antiproliferative activity against HepG2, which is 6-fold more potent than Vorinostat. Molecular docking analysis showed that the phenyl group with a small substituent group is crucial for HDAC6 selectivity. This study provides further possibility of developing HDAC6 selectivity inhibitors for the treatment of cancer.

4. Experimental section

4.1 Chemistry

The melting points were determined on an electrically heated X-4 digital visual melting point apparatus and were uncorrected. Mass spectra (MS) were determined on a Finnigan MAT/USA spectrometer (LC-MS). ^{1}H NMR and ^{13}C NMR spectrum were recorded on Bruker AV-400 or ARX 600 spectrometers with tetramethylsilane (TMS) used as the internal standard. Chemical shifts were reported in ppm (δ). High–resolution mass spectra were obtained on Bruker

microTOF–Q in the ESI mode (HR–ESI–MS). All reactions were performed with commercially available reagents and they were used without further purification. All reactions were monitored by thin-layer chromatography (TLC) carried on fluorescent precoated plates GF254 (Qindao Haiyang Chemical, China) and detection of the components was made by short UV light. Column chromatography was performed with silica gel 60 (200–300 mesh).

4.1.1 The synthesis of *N*-hydroxy-4-(5-(*p*-tolyl)-3-(trifluoromethyl)-1*H*-pyrazol-1-yl)benzamide (8)

A solution of p-methylacetophenone (0.67 g, 5 mmol) in dry THF (20 mL) was added dropwise to NaH (0.24 g, 10 mmol) in dry THF (50 mL) under nitrogen atomosphere and the mixture was stirred for 1h at 0^{o}C. Then a solution of ethyl trifluoroacetate (0.9mL, 7.5 mmol) in dry THF (10 mL) was added dropwise. The mixture was warmed to room temperature for 12h. The reaction was quenched with saturation $NaHCO_3$ and extracted with ethyl acetate (50 mL × 3). The combined organic extracts were washed with brine (50 mL), dried with Na_2SO_4 and evaporated. Finally, the resulting residue was purified by column chromatography on silica gel as indicated to give **6a** as canary yellow solid.

To a solution of 6a (0.46 g, 2 mmol) in ethyl alcohol (50 mL) was added 4-hydrazinyl-*N*-hydroxybenzamide hydrochloride (0.53 g, 2.6 mmol). Then the temperature was raised to 70^{o}C for 5h. The mixture solution was concentrated to dryness, added water (50 mL) and extracted with ethyl acetate (30 mL × 3). The combined organic extracts were washed with brine (30 mL), dried with Na_2SO_4 and concentrated. Finally, the resulting residue was purified by column chromatography on silica gel as indicated to give **7** as white solid.

To a solution of 7 (0.36 g, 1 mmol) in methyl alcohol (30 mL) were added 1 M aqueous solution of NaOH (3 mL) and NH_2OH (50 wt % in water, 3 mL) dropwise successively at 0^{o}C. The reaction was warmed to room temperature for 3h. The mixture solution was concentrated to dryness, and the obtained solid was dissolved in water. The pH was adjusted to 7 with 1M aqueous solution of HCl. The resulting precipitate was filtered to give **8** as white solid. Yield: 63.2%. Mp: 104.5-105.9°C. ESI-MS: m/z, 360.3 $[M-H]^-$. ^{1}H-NMR (600 MHz, DMSO-d_6) δ: 11.33 (s, 1H), 9.13 (s, 1H), 7.80 (d, J = 8.6 Hz, 2H), 7.42 (d, J = 8.6 Hz, 2H), 7.21 – 7.18 (m, 4H), 7.17 (s, 1H), 2.30 (s, 3H). ^{13}C-NMR (151 MHz, DMSO) δ: 145.19, 140.87, 139.03, 132.90, 129.56, 129.43, 128.77, 128.00, 126.86, 125.60, 125.54, 105.91, 20.86. .

HRMS (ESI+) *m/z* calcd for $C_{18}H_{14}F_3N_3O_2$ $[M-H]^-$ 360.1038, found: 360.1047.

4.1.2 General procedure for the synthesis of 11a-11p

Compounds **6b-6g** were synthesized from **5a-5c** with appropriate carboxylic ethyl ether by the synthetic method of **6a**.

To a solution of **6a-6g** (10 mmol) in acetic acid (50 mL) was added hydrazine hydrate (0.76 g, 11 mmol). The temperature was raised to 80°C for 4 h. When the mixture was cooled to room temperature, the resulting solution was poured into water (100 mL) and extracted with ethyl acetate (50 mL × 3). The combined organic extracts were washed with brine (50 mL), dried with Na_2SO_4 and concentrated. Finally, the resulting residue was purified by column chromatography on silica gel as indicated to give **9a-9g**.

To a solution of **9a-9g** (5 mmol) in acetonitrile (100 mL) was added methyl 4-(bromomethyl)benzoate (1.37 g, 6 mmol) or methyl 4-(2-bromoethyl)benzoate (1.46 g, 6mmol). Then Cs_2CO_3 (3.26 g, 10 mmol) was added and the temperature was raised to 70^{o}C for 5h. The mixture solution was concentrated to dryness, added water (100 mL) and extracted with ethyl acetate (80 mL × 3). Finally, the organic layers were combined, washed with brine, dried with Na_2SO_4 and evaporated. Finally, the resulting residue was purified by column chromatography on silica gel as indicated to give **10a-10p** as white solid.

To a solution of **10a-10p** (1 mmol) in methyl alcohol (30 mL) were added 1 M aqueous solution of NaOH (3 mL) and NH_2OH (50 wt % in water, 3 mL) dropwise successively at 0^{o}C. The reaction was warmed to room temperature for 3h. The mixture solution was concentrated to dryness, and the obtained solid was dissolved in water (10 mL). The pH was adjusted to 7 with a 1M aqueous solution of HCl. The resulting precipitate was filtered to give **11a-1p** as white solid.

4.1.2.1 *N*-hydroxy-4-((5-(*p*-tolyl)-3-(trifluoromethyl)-1*H*-pyrazol-1-yl)methyl)benzamide (11a)

Yield: 27.1%. Mp: 171.7-173.8°C. ESI-MS: m/z, 374.2 $[M-H]^-$. ^{1}H-NMR (600 MHz, DMSO-d_6) δ: 11.17 (s, 1H), 9.02 (s, 1H), 7.67 (d, *J* = 8.3 Hz, 2H), 7.36 (d, *J* = 8.1 Hz, 2H), 7.30 (d, *J* = 7.9 Hz, 2H), 7.05 (d, *J* = 8.3 Hz, 2H), 6.94

(s, 1H), 5.50 (s, 2H), 2.34 (s, 3H). ^{13}C-NMR (101 MHz, DMSO) δ: 164.26, 146.07, 140.06, 139.62, 132.65, 130.03, 129.14, 127.76, 127.10, 126.04, 105.25, 53.47, 21.29. HRMS (ESI+) *m/z* calcd for $C_{19}H_{16}F_3N_3O_2$ $[M-H]^-$ 374.1195, found: 374.1187.

4.1.2.2 *N*-hydroxy-4-((3-(*p*-tolyl)-5-(trifluoromethyl)-1*H*-pyrazol-1-yl)methyl)benzamide (11b)

Yield: 41.5%. Mp: 152.6-153.8°C. ESI-MS: m/z, 374.1 $[M-H]^-$. ^{1}H-NMR (600 MHz, DMSO-d_6) δ: 10.99 (s, 1H), 9.05 (s, 1H), 7.77 (m, 1H), 7.76 (m, 1H), 7.73 (m, 1H), 7.71 (m, 1H), 7.26 – 7.24 (m, 4H), 7.24 (s, 1H), 5.57 (s, 2H), 2.33 (s, 3H). ^{13}C-NMR (151 MHz, DMSO) δ: 150.51, 139.41, 138.04, 132.46, 129.65, 129.48, 128.77, 127.33, 126.88, 126.72, 125.43, 105.55, 53.91, 20.92. HRMS (ESI+) *m/z* calcd for $C_{19}H_{16}F_3N_3O_2$ $[M-H]^-$ 374.1195, found: 374.1195.

4.1.2.3 *N*-hydroxy-4-(2-(5-(*p*-tolyl)-3-(trifluoromethyl)-1*H*-pyrazol-1-yl)ethyl)benzamide (11c)

Yield: 25.4%. Mp: 98.7-99.8°C. ESI-MS: m/z, 388.3 $[M-H]^-$. ^{1}H-NMR (600 MHz, DMSO-d_6) δ: 11.14 (s, 1H), 8.98 (s, 1H), 7.59 (d, J = 8.2 Hz, 2H), 7.26 (s, 1H), 7.25 (s, 1H), 7.15 (d, J = 8.0 Hz, 2H), 7.04 (d, J = 8.2 Hz, 2H), 6.75 (s, 1H), 4.37 (t, J = 7.2 Hz, 2H), 3.10 (t, J = 7.2 Hz, 2H), 2.35 (s, 3H). ^{13}C-NMR (101 MHz, DMSO-d_6) δ: 150.42, 141.46, 138.25, 132.50, 131.56, 129.84, 129.66, 129.40, 129.19, 128.89, 127.42, 125.77, 105.14, 52.09, 35.86, 21.31. HRMS (ESI+) *m/z* calcd for $C_{20}H_{18}F_3N_3O_2$ $[M-H]^-$ 388.1357, found: 388.1387.

4.1.2.4 *N*-hydroxy-4-(2-(3-(*p*-tolyl)-5-(trifluoromethyl)-1*H*-pyrazol-1-yl)ethyl)benzamide (11d)

Yield: 40.1%. Mp: 78.6-79.8°C. ESI-MS: m/z, 388.2 $[M-H]^-$. ^{1}H-NMR (600 MHz, DMSO) δ: 11.15 (s, 1H), 8.99 (s, 1H), 7.75 (d, J = 8.0 Hz, 2H), 7.65 (d, J = 8.2 Hz, 2H), 7.31 (s, 1H), 7.26 (s, 1H), 7.24 (d, J = 3.0 Hz, 2H), 7.23 (s, 1H), 4.47 (t, J = 7.2 Hz, 2H), 3.24 (t, J = 7.1 Hz, 2H), 2.33 (s, 3H). ^{13}C-NMR (101 MHz, DMSO-d_6) δ: 145.77, 141.48, 139.35, 131.58, 129.83, 129.79, 129.37, 129.21, 129.12, 129.02, 127.38, 126.16, 104.68, 51.11, 35.55, 21.29. HRMS (ESI+) *m/z* calcd for $C_{20}H_{18}F_3N_3O_2$ $[M-H]^-$ 388.1357, found:388.1275.

4.1.2.5 *N*-hydroxy-4-(3-methyl-5-(*p*-tolyl)-1*H*-pyrazol-1-yl)benzamide (11e)

Yield: 29.8%. Mp: 110.5-111.9°C. ESI-MS: m/z, 320.1 $[M-H]^-$. ^{1}H-NMR (600 MHz, DMSO-d_6) δ: 11.15 (s, 1H), 9.00 (s, 1H), 7.65 (d, *J* = 8.3 Hz, 2H), 7.25 (q, *J* = 8.2 Hz, 4H), 7.03 (d, *J* = 8.3 Hz, 2H), 6.21 (s, 1H), 5.30 (s, 2H), 2.32

(s, 3H), 2.20 (s, 3H). ^{13}C-NMR (151 MHz, DMSO-d6) δ: 164.31, 147.58, 144.59, 141.65, 138.36, 132.12, 129.77, 128.55, 127.72, 127.48, 126.77, 106.16, 52.24, 21.15, 13.74. HRMS (ESI+) *m/z* calcd for $C_{19}H_{19}N_3O_2$ $[M-H]^-$ 320.1477, found: 320.1476.

4.1.2.6 *N*-hydroxy-4-(5-methyl-3-(*p*-tolyl)-1*H*-pyrazol-1-yl)benzamide (11f)

Yield: 44.0%. Mp: 125.8-127.6°C. ESI-MS: m/z, 320.3 $[M-H]^-$. ^{1}H-NMR (600 MHz, DMSO-d_6) δ: 11.17 (s, 1H), 9.01 (s, 1H), 7.71 (d, *J* = 8.3 Hz, 2H), 7.64 (d, *J* = 8.1 Hz, 2H), 7.19 (t, *J* = 7.9 Hz, 4H), 6.51 (s, 1H), 5.37 (s, 2H), 2.30 (s, 3H), 2.24 (s, 3H). ^{13}C-NMR (151 MHz, DMSO-d6) δ: 163.95, 149.33, 140.81, 140.06, 136.59, 131.99, 130.79, 129.23, 127.31, 126.85, 124.98, 102.72, 51.80, 20.89, 10.89. HRMS (ESI+) *m/z* calcd for $C_{19}H_{19}N_3O_2$ $[M-H]^-$ 320.1477, found: 320.1477.

4.1.2.7 4-(5-(benzo[*d*][1,3]dioxol-5-yl)-3-methyl-1H-pyrazol-1-yl)-*N*-hydroxybenzamide (11g)

Yield: 25.7%. Mp: 175.3-176.7°C. ESI-MS: m/z, 350.1 $[M-H]^-$. ^{1}H-NMR (600 MHz, DMSO-d_6) δ: 11.12 (s, 1H), 9.01 (s, 1H), 7.83 (d, J = 8.1 Hz, 1H), 7.65 (d, J = 8.3 Hz, 2H), 7.03 (d, J = 8.2 Hz, 2H), 6.96 (d, J = 8.0 Hz, 1H), 6.92 (d, J = 1.6 Hz, 1H), 6.83 (d, J = 1.7 Hz, 1H), 6.82 (d, J = 1.7 Hz, 1H), 6.19 (s, 1H), 6.05 (s, 2H), 5.29 (s, 2H), 2.18 (s, 3H).. ^{13}C-NMR (101 MHz, DMSO-d_6) δ: 164.21, 148.00, 147.55, 144.37, 141.70, 132.22, 129.93, 127.56, 126.88, 126.76, 124.34, 122.68, 109.16, 109.06, 106.36, 101.86, 52.32, 13.83. HRMS (ESI+) *m/z* calcd for $C_{19}H_{17}N_3O_4$ $[M-H]^-$ 350.1219, found: 350.1311.

4.1.2.8 4-(3-(benzo[*d*][1,3]dioxol-5-yl)-5-methyl-1*H*-pyrazol-1-yl)-*N*-hydroxybenzamide (11h)

Yield: 43.5%. Mp: 151.8-153.1°C. ESI-MS: m/z, 350.3 $[M-H]^-$. ^{1}H-NMR (600 MHz, DMSO-d_6) δ: 11.15 (s, 1H), 9.03 (s, 1H), 7.71 (d, *J* = 8.3 Hz, 2H), 7.27 (dd, *J* = 16.2, 5.6 Hz, 2H), 7.19 (d, *J* = 8.2 Hz, 2H), 6.91 (d, *J* = 8.0 Hz, 1H), 6.48 (s, 1H), 6.02 (s, 2H), 5.36 (s, 2H), 2.22 (s, 3H). ^{13}C-NMR (151 MHz, DMSO-d_6) δ: 163.96, 149.10, 147.67, 146.66, 140.74, 140.06, 132.02, 127.89, 127.28, 126.84, 118.63, 108.51, 105.44, 102.68, 101.00, 51.76, 10.88. HRMS (ESI+) *m/z* calcd for $C_{19}H_{17}N_3O_4$ $[M-H]^-$ 350.1219, found: 350.1217.

4.1.2.9 4-(5-(4-fluorophenyl)-3-methyl-1*H*-pyrazol-1-yl)-*N*-hydroxybenzamide (11i)

Yield: 22.4%. Mp: 142.5-144.1°C. ESI-MS: m/z, 324.1 $[M-H]^-$. ^{1}H-NMR (400 MHz, DMSO-d_6) δ: 11.16 (s, 1H), 9.04 (s, 1H), 7.65 (d, J = 8.1 Hz, 2H), 7.41 (dd, J = 8.5, 5.5 Hz, 2H), 7.27 (t, J = 8.8 Hz, 2H), 7.02 (d, J = 8.1 Hz, 2H), 6.25 (s, 1H), 5.30 (s, 2H), 2.20 (s, 3H). ^{13}C-NMR (101 MHz, DMSO-d_6) δ: 163.86, 162.90, 160.47, 148.41, 140.53, 140.34, 132.22, 130.12, 130.10, 127.27, 127.00, 126.92, 126.84, 115.63, 115.42, 102.91, 51.85, 10.90. HRMS (ESI+) *m*/*z* calcd for $C_{18}H_{16}FN_3O_2$ $[M-H]^-$ 324.1227, found: 324.1154.

4.1.2.10 4-(3-(4-fluorophenyl)-5-methyl-1*H*-pyrazol-1-yl)-*N*-hydroxybenzamide (11j)

Yield: 40.1%. Mp: 178.3-178.9°C. ESI-MS: m/z, 324.2 $[M-H]^-$. ^{1}H-NMR (400 MHz, DMSO-d_6) δ: 11.19 (s, 1H), 9.03 (s, 1H), 7.79 (dd, *J* = 8.7, 5.6 Hz, 2H), 7.71 (d, *J* = 8.2 Hz, 2H), 7.21 (t, *J* = 8.3 Hz, 4H), 6.55 (s, 1H), 5.39 (s, 2H), 2.24 (s, 3H). ^{13}C-NMR (101 MHz, DMSO-d_6) δ: 163.97, 163.38, 160.93, 147.31, 143.20, 141.14, 131.86, 130.67, 130.59, 127.20, 126.80, 126.77, 126.53, 116.01, 115.80, 106.30, 52.01, 13.42.. HRMS (ESI+) *m*/*z* calcd for $C_{18}H_{16}FN_3O_2$ $[M-H]^-$ 324.1227, found: 324.1206.

4.1.2.11 4-(3-ethyl-5-(4-fluorophenyl)-1*H*-pyrazol-1-yl)-*N*-hydroxybenzamide (11k)

Yield: 23.3%. Mp: 169.2-171.1°C. ESI-MS: m/z, 338.1 $[M-H]^-$. ^{1}H NMR (600 MHz, DMSO) δ: 11.12 (s, 1H), 9.02 (s, 1H), 7.65 (d, J = 8.3 Hz, 2H), 7.44 – 7.40 (m, 2H), 7.29 – 7.25 (m, 2H), 7.01 (d, J = 8.3 Hz, 2H), 6.29 (s, 1H), 5.32 (s, 2H), 2.58 (q, J = 7.6 Hz, 2H), 1.20 (t, J = 7.6 Hz, 3H).. ^{13}C-NMR (101 MHz, DMSO-d_6) δ: 163.87, 163.36, 160.91, 144.73, 143.07, 141.16, 131.87, 130.67, 130.59, 127.18, 126.89, 126.86, 126.49, 116.00, 115.79, 104.89, 52.08, 21.03, 13.82.. HRMS (ESI+) *m*/*z* calcd for $C_{19}H_{18}FN_3O_2$ $[M-H]^-$ 338.1383, found: 338.1308.

4.1.2.12 4-(5-ethyl-3-(4-fluorophenyl)-1*H*-pyrazol-1-yl)-*N*-hydroxybenzamide (11l)

Yield: 39.5%. Mp: 166.3-167.5°C. ESI-MS: m/z, 338.2 $[M-H]^-$. ^{1}H-NMR (600 MHz, DMSO-d_6) δ: 11.17 (s, 1H), 9.01 (s, 1H), 7.81 (dd, *J* = 8.5, 5.7 Hz, 2H), 7.70 (d, *J* = 8.2 Hz, 2H), 7.23 – 7.17 (m, 4H), 6.59 (s, 1H), 5.39 (s, 2H), 2.58 (q, *J* = 7.5 Hz, 2H), 1.17 (t, *J* = 7.5 Hz, 3H). ^{13}C-NMR (101 MHz, DMSO-d_6) δ: 164.02, 162.89, 160.47, 148.46, 146.42, 140.82, 132.00, 130.17, 130.14, 127.30, 127.01, 126.93, 126.82, 115.62, 115.41, 101.22, 51.77, 18.31, 12.78. HRMS (ESI+) *m*/*z* calcd for $C_{19}H_{18}FN_3O_2$ $[M-H]^-$ 338.1383, found: 338.1384.

4.1.2.13 4-(5-(4-fluorophenyl)-3-propyl-1*H*-pyrazol-1-yl)-*N*-hydroxybenzamide (11m)

Yield: 26.4%. Mp: 150.1-151.5°C. ESI-MS: m/z, 352.1 $[M-H]^-$. ^{1}H NMR (600 MHz, DMSO) δ: 11.14 (s, 1H), 8.99 (s, 1H), 7.64 (d, J = 8.2 Hz, 2H), 7.43 – 7.40 (m, 2H), 7.28 – 7.24 (m, 2H), 7.00 (d, J = 8.2 Hz, 2H), 6.28 (s, 1H), 5.32 (s, 2H), 2.53 (t, J = 7.5 Hz, 2H), 1.67 – 1.60 (m, 2H), 0.94 (t, J = 7.4 Hz, 3H). ^{13}C-NMR (101 MHz, DMSO-d_6) δ: 163.95, 163.34, 160.90, 147.16, 143.05, 141.25, 131.82, 130.65, 129.63, 127.18, 126.83, 126.56, 126.41, 115.99, 115.77, 105.35, 52.06, 29.80, 22.38, 13.92. HRMS (ESI+) *m*/*z* calcd for $C_{20}H_{20}FN_3O_2$ $[M-H]^-$ 352.1540, found: 352.1445.

4.1.2.14 4-(3-(4-fluorophenyl)-5-propyl-1*H*-pyrazol-1-yl)-*N*-hydroxybenzamide (11n)

Yield: 44.3%. Mp: 170.2-170.8°C. ESI-MS: m/z, 352.2 $[M-H]^-$. ^{1}H-NMR (400 MHz, DMSO-d_6) δ: 11.17 (s, 1H), 9.02 (s, 1H), 7.81 (dd, *J* = 8.8, 5.6 Hz, 2H), 7.70 (d, *J* = 8.2 Hz, 2H), 7.24 – 7.16 (m, 4H), 6.59 (s, 1H), 5.40 (s, 2H), 2.55 (t, *J* = 7.6 Hz, 2H), 1.63 – 1.51 (m, 2H), 0.90 (t, *J* = 7.3 Hz, 3H). ^{13}C-NMR (101 MHz, DMSO-d_6) δ: 164.02, 162.89, 160.47, 148.47, 144.89, 141.00, 131.97, 130.14, 129.74, 127.28, 127.02, 126.94, 126.77, 115.62, 115.41, 101.78, 51.75, 26.83, 21.48, 13.73. HRMS (ESI+) *m*/*z* calcd for $C_{20}H_{20}FN_3O_2$ $[M-H]^-$ 352.1540, found: 352.1547.

4.1.2.15 4-(3-benzyl-5-(4-fluorophenyl)-1*H*-pyrazol-1-yl)-*N*-hydroxybenzamide (11o)

Yield: 21.6%. Mp: 115.4-117.6°C. ESI-MS: m/z, 400.1 $[M-H]^-$. ^{1}H NMR (600 MHz, DMSO) δ 11.15 (s, 1H), 9.02 (s, 1H), 7.84 (d, J = 8.2 Hz, 1H), 7.65 (d, J = 8.3 Hz, 2H), 7.42 – 7.39 (m, 2H), 7.30 (d, J = 1.4 Hz, 2H), 7.29 (s, 2H), 7.27 – 7.24 (m, 2H), 7.02 (d, J = 8.2 Hz, 2H), 6.25 (s, 1H), 5.35 (s, 2H), 3.92 (s, 2H).. ^{13}C-NMR (101 MHz, DMSO-d_6) δ: 163.85, 163.39, 160.94, 151.02, 143.35, 141.07, 140.09, 131.89, 130.69, 130.61, 128.68, 128.44, 127.19, 126.64, 126.47, 126.30, 126.11, 116.01, 115.79, 105.92, 52.17, 34.06. HRMS (ESI+) *m*/*z* calcd for $C_{24}H_{20}FN_3O_2$ $[M-H]^-$ 400.1540, found: 400.1450.

4.1.2.16 4-(5-benzyl-3-(4-fluorophenyl)-1*H*-pyrazol-1-yl)-*N*-hydroxybenzamide (11p)

Yield: 38.3%. Mp: 179.5-181.3°C. ESI-MS: m/z, 400.3 $[M-H]^-$. ^{1}H-NMR (600 MHz, DMSO-d_6) δ: 11.17 (s, 1H), 9.01 (s, 1H), 7.87 (d, J = 8.4 Hz, 1H), 7.78 (dd, J = 6.1, 2.8 Hz, 2H), 7.66 (d, J = 8.3 Hz, 2H), 7.29 – 7.26 (m, 2H), 7.21 – 7.19 (m, 2H), 7.19 (t, J = 1.8 Hz, 2H), 7.13 (d, J = 8.3 Hz, 2H), 6.50 (s, 1H), 5.37 (s, 2H), 4.02 (s, 2H). ^{13}C-NMR (101

MHz, DMSO-d_6) δ: 163.96, 162.94, 160.51, 148.64, 143.85, 140.54, 137.94, 131.95, 129.88, 129.46, 128.68, 128.65, 127.18, 127.07, 126.99, 126.61, 115.64, 115.43, 103.16, 51.93, 30.97. HRMS (ESI+) *m*/*z* calcd for $C_{24}H_{20}FN_3O_2$ $[M-H]^-$ 400.1540, found: 400.1565.

4.1.3 **General procedure for the synthesis of 16a-16f**

To a solution of 1-(4-fluorophenyl)ethanone (1.38 g, 10mmol) and dimethyl oxalate (1.18 g, 10mmol) in diethyl ether (150 mL) was added dropwise NaOMe (0.65 g, 12mmol) in MeOH (20 mL). The mixture was stirred for 12h at room temperature and then filtrated under reduced pressure to give **12**.

To a solution of **12** (2.24 g, 10 mmol) in acetic acid (50 mL) was added hydrazine hydrate (0.76 g, 11 mmol). The temperature was raised to 80°C for 4 h. When the mixture was cooled to room temperature, the resulting solution was poured into water (100 mL). The resulting precipitate was then hydrolyzed into carboxylic acids **14** with sodium hydroxide (12 mmol) in 50°C for 4 h. Acidify the mixture to pH 2 with 2M HCl, the precipitate was filtered under reduced pressure.

To a solution of **14** (1.03 g, 5 mmol) in THF (20 mL) were added 1-ethyl-3-(3-dimethylamino-propyl)carbodiimide (EDCI, 1.15 g, 6 mmol), 1-hydroxy-1*H*-benzotriazole (HOBt, 0.81 g, 6mmol) and appropriate amino acid methyl ester hydrochloride (6 mmol). The mixture was stirred at room temperature for 24 h and then poured into water (100 mL), extracted with ethyl acetate (50 mL × 3). Finally, the organic layers were combined, washed with brine, dried with Na_2SO_4 and evaporated. Finally, the resulting residue was purified by column chromatography on silica gel as indicated to give **15a-15f** as white solid.

To a solution of **15a-15f** (1 mmol) in methyl alcohol (30 mL) were added 1 M aqueous solution of NaOH (3 mL) and NH_2OH (50 wt % in water, 3 mL) dropwise successively at 0^oC. The reaction was warmed to room temperature for 3h. The mixture solution was concentrated to dryness, and the obtained solid was dissolved in water (10 mL). The pH was adjusted to 7 with a 1M aqueous solution of HCl. The resulting precipitate was filtered under reduced pressure to give **16a-16f** as white solid.

4.1.3.1 5-(4-fluorophenyl)-*N*-(4-(hydroxycarbamoyl)benzyl)-1*H*-pyrazole-3-carboxamide (16a)

Yield: 54.8%. Mp: 245.2-247.5°C. ESI-MS: m/z, 353.1 $[M-H]^-$. ^{1}H-NMR (600 MHz, DMSO-d_6) δ: 13.70 (s, 1H), 11.17 (s, 1H), 8.99 (s, 1H), 8.83 (s, 1H), 7.84 (s, 2H), 7.70 (s, 2H), 7.38 (d, J = 6.6 Hz, 2H), 7.31 (d, J = 4.9 Hz, 2H), 7.07 (s, 1H), 4.49 (s, 2H). ^{13}C-NMR (101 MHz, DMSO-d_6) δ: 164.51, 163.62, 161.19, 143.28, 131.76, 129.75, 128.86, 127.82, 127.56, 127.37, 127.32, 116.47, 116.25, 114.14, 103.02, 42.24. HRMS (ESI+) *m*/*z* calcd for 353.1040.

4.1.3.2 5-(4-fluorophenyl)-*N*-(3-(hydroxyamino)-3-oxopropyl)-1*H*-pyrazole-3-carboxamide (16b)

Yield: 57.9%. Mp: 192.7-193.5°C. ESI-MS: m/z, 291.0 $[M-H]^-$. ^{1}H-NMR (600 MHz, DMSO-d_6) δ: 13.62 (s, 1H), 10.47 (s, 1H), 8.76 (s, 1H), 8.13 (t, *J* = 4.7 Hz, 1H), 7.85 (d, *J* = 6.5 Hz, 1H), 7.79 (d, *J* = 4.4 Hz, 1H), 7.33 (d, *J* = 8.6 Hz, 1H), 7.27 (d, *J* = 8.1 Hz, 1H), 7.05 (s, 1H), 3.45 (dd, *J* = 12.4, 6.2 Hz, 2H), 2.26 (t, *J* = 6.2 Hz, 2H). ^{13}C-NMR NMR (101 MHz, DMSO) δ: 167.59, 161.59, 160.89, 147.87, 142.66, 127.64, 127.57, 127.07, 116.22, 116.01, 102.71, 35.31, 32.45. HRMS (ESI+) *m*/*z* calcd for $C_{13}H_{13}FN_4O_3$ $[M-H]^-$ 291.0972, found: 291.0899.

4.1.3.3 5-(4-fluorophenyl)-*N*-(4-(hydroxyamino)-4-oxobutyl)-1*H*-pyrazole-3-carboxamide (16c)

Yield: 55.3%. Mp: 142.5-143.1°C. ESI-MS: m/z, 305.1 $[M-H]^-$. ^{1}H-NMR (600 MHz, DMSO-d_6) δ: 13.63 (s, 1H), 10.40 (s, 1H), 8.72 (s, 1H), 8.23 (s, 1H), 7.83 (s, 2H), 7.30 (s, 2H), 7.05 (s, 1H), 3.24 (dd, *J* = 12.8, 6.5 Hz, 2H), 2.07 – 1.94 (m, 2H), 1.78 – 1.70 (m, 2H). ^{13}C-NMR (101 MHz, DMSO) δ: 168.94, 163.20, 160.78, 147.71, 142.44, 127.47, 127.43, 127.14, 116.08, 115.88, 102.62, 38.30, 30.08, 25.53.. HRMS (ESI+) *m*/*z* calcd for $C_{14}H_{15}FN_4O_3$ $[M-H]^-$ 305.1128, found: 305.1097.

4.1.3.4 5-(4-fluorophenyl)-*N*-(5-(hydroxyamino)-5-oxopentyl)-1*H*-pyrazole-3-carboxamide (16d)

Yield: 50.6%. Mp: 107.9-108.6°C. ESI-MS: m/z, 319.1 $[M-H]^-$. ^{1}H-NMR (600 MHz, DMSO-d_6) δ: 13.59 (s, 1H), 10.34 (s, 1H), 8.66 (s, 1H), 8.16 (s, 1H), 7.82 (d, *J* = 27.0 Hz, 3H), 7.29 (d, *J* = 35.7 Hz, 3H), 7.03 (s, 1H), 3.23 (d, *J* = 5.4 Hz, 2H), 2.04 – 1.93 (s, 2H), 1.58 – 1.44 (s, 5H). ^{13}C-NMR (101 MHz, DMSO-d_6) δ: 169.10, 161.57, 158.63, 148.10, 142.57, 127.61, 127.57, 127.08, 116.21, 116.00, 102.70, 38.17, 32.11, 29.08, 22.78. HRMS (ESI+) *m*/*z* calcd for $C_{15}H_{17}FN_4O_3$ $[M-H]^-$ 319.1285, found: 319.1260.

4.1.3.5 5-(4-fluorophenyl)-*N*-(6-(hydroxyamino)-6-oxohexyl)-1*H*-pyrazole-3-carboxamide (16e)

Yield: 49.7%. Mp: 114.2-115.0°C. ESI-MS: m/z, 333.2 $[M-H]^-$. ^{1}H-NMR (600 MHz, DMSO-d_6) δ: 13.59 (s, 1H), 10.33 (s, 1H), 8.65 (s, 1H), 8.13 (s, 1H), 7.83 (s, 2H), 7.30 (s, 2H), 7.03 (s, 1H), 3.23 (s, 2H), 1.95 (t, J = 7.3 Hz, 2H), 1.54 – 1.48 (m, 4H), 1.27 (s, 2H). ^{13}C-NMR (101 MHz, DMSO-d_6) δ: 169.17, 162.83, 161.23, 148.15, 142.56, 127.59, 127.33, 127.07, 116.10, 116.01, 102.72, 38.48, 32.34, 29.17, 26.17, 25.02. HRMS (ESI+) *m*/*z* calcd for $C_{16}H_{19}FN_4O_3$ $[M-H]^-$ 333.1441, found: 333.1368.

4.1.3.6 5-(4-fluorophenyl)-*N*-(7-(hydroxyamino)-7-oxoheptyl)-1*H*-pyrazole-3-carboxamide (16f)

Yield: 53.3%. Mp: 92.5-93.7°C. ESI-MS: m/z, 347.1 $[M-H]^-$. ^{1}H-NMR (600 MHz, DMSO-d_6) δ: 13.59 (s, 1H), 10.33 (s, 1H), 8.65 (s, 1H), 8.13 (s, 1H), 7.83 (s, 2H), 7.30 (s, 2H), 7.03 (s, 1H), 3.23 (s, 2H), 1.95 (t, J = 7.3 Hz, 2H), 1.54 – 1.48 (m, 4H), 1.27 (s, 2H). ^{13}C-NMR (101 MHz, DMSO-d_6) δ: 169.18, 163.17, 160.75, 147.57, 142.55, 127.46, 127.37, 127.08, 116.06, 115.85, 102.65, 38.55, 32.32, 29.21, 28.43, 26.27, 25.19.. HRMS (ESI+) *m*/*z* calcd for $C_{17}H_{21}FN_4O_3$ $[M-H]^-$ 347.1598, found: 347.1518.

4.2. Biological assays

4.2.1 HDAC inhibition fluorescence assay

In this HDACs assay, HeLa nuclear extracts (Enzo Life Sciences, USA) were used as a source of histone deacetylase. The recombinant human HDAC1, 2, 3, 6 and 8 were purchased from BPS Bioscience (USA). All reactions were performed in the black half area 96–well microplates. A serial dilution of the inhibitors (5 µL/well) and enzymes (5 µL/well) were pre-incubated in HDAC buffer (10 µL/well) at 25°C for 15 min, and then fluorogenic substrate (5 µL/well) Boc–Lys(Ac)–AMC (for HeLa NuEx, HDAC1, 2, 3 and 6 isoforms) or Boc–Lys(TFA)–AMC (for HDAC 8 isoform) was added. After incubation at 37°C for 60 min, the mixture was stopped by the addition of developer (25 µL/well) for 10 min. Fluorescence intensity was measured using the Thermo Scientific Varioskan Flash Station at excitation and emission wavelengths of 355 (or 360 for the HeLa NuEx) and 460 nm, respectively. The IC_{50} values were extracted by curve fitting the dose/response slopes.

4.2.2 Anti-proliferative assays

Cells were provided by the Shanghai Cell Bank, Chinese Academy of Sciences. The cells were cultured in media, DMEM (High Glucose) for A549, MEM for HepG2 with 10% FBS and antibiotics (100 units/mL penicillin G sodium and 100 ng/mL streptomycin). All cells were incubated in a Thermo/Forma Scientific CO_2 water jacketed incubator with 5% CO_2 in air at 37°C. The anti-proliferative activities of target compounds were evaluated by the methyl thiazolyl tetrazolium bromide (MTT) assay. Cells ($1.5\text{-}3.5\times10^4$ cells/well in 100 μL medium) were incubated for 24 h, then various concentrations of each compound mixed in 100 μL medium were added to each well. After another 96 h of incubation at 37°C, MTT solution (50 μL of 2 mg/mL) was added per well and the cultures were continued for an additional 4 h. The medium was removed by aspiration and the cells were dissolved in 200 μL DMSO. The absorbance at 570 nm was measured in the 96-well plate reader. Growth inhibition was calculated and expressed as the ratio of the cell number in the treated group to that of the untreated group. The GI_{50} values were calculated according to inhibition ratios.

Acknowledgment

This work was supported by the National Nature Science Foundation of China (No. 81473086), Nature Science Foundation of Liaoning Province (No. 2015020728-301).

References and notes

[1] Witt, O.; Deubzer, H. E.; Milde, T.; Oehme, I. *Cancer Lett*. **2009**, *277*, 8-21.

[2] Minucci, S.; Pelicci, P. G. *Nat. Rev. Cancer*. **2006**, *6*, 38-51.

[3] Kalin, J. H.; Bergman, J. A. *J. Med. Chem.* **2013**, *56*, 6297-313.

[4] Weichert W. *Cancer Lett*. **2009**, *280*, 168-76.

[5] Marks, P. A.; Breslow, R. *Nat. Biotechnol*. **2007**, *25*, 84-90.

[6] Yang, L. P. H. *Drugs*. **2011**, *71*, 1469-80.

[7] Poole, R. M. *Drugs*. **2014**, *74*, 1543-54.

[8] Garnock-Jones, K. P. *Drugs*. **2015**, *75*, 695-704.

[9] Chan, T. S.; Tse, E.; Kwong, Y. L. *OncoTargets Ther*. **2017**, *10*, 347-52.

[10] Fraczek, J.; Vanhaecke, T.; Rogiers, V. *Expert Opin Drug Met*. **2013**, *9*, 441-57.

[11] Seidel, C.; Schnekenburger, M.; Dicato, M.; Diederich, M. *Epigenomics*. **2015**, *7*, 103-18.

[12] Krämer, O. H.; Mahboobi, S.; Sellmer, A. *Trends Pharmacol. Sci*. **2014**, *35*, 501-9.

[13] Ai, T.; Qiu, L.; Xie, J. S.; Geraghty, R. J.; Chen, L. Q. *Bioorg. Med. Chem.* **2016**, *24*, 686-92.

[14] Zhang, L.; Sheng, S. l.; Qin, C. *J. Alzheimers Dis.* **2013**, *33*, 283-95.

[15] Tapadar, S.; Fathi, S.; Raji, I.; Omesiete, W.; Kornacki, J. R.; Mwakwari, S. C.; Miyata, M.; Mitsutake, K.; Li, J. D.; Mrksich, M.; Oyelere, A. K. *Bioorg. Med. Chem*. **2015**, *23*, 7543-64.

[16] Ding, C.; Chen, S.; Zhang, C.; Hu, G.; Zhang, W.; Li, L.; Chen, Y. Z.; Tan, C.; Jiang, Y. *Bioorg. Med. Chem.* **2017**, *25*, 27-37.

[17] Parmigiani, R. B.; Xu, W. S.; Venta-Perez, G.; Erdjument-Bromage, H.; Yaneva, M.; Tempst, P.; Marks, P. A. P. *Natl. Acad. Sci. U.S.A*. **2008**, *105*, 9633-8.

[18] Wong, J. C.; Hong, R.; Schreiber, S. L. *J. Am. Chem. Soc*. **2003**, *125*, 5586-7.

[19] Yee, A. J.; Bensinger, W. I.; Supko, J. R. G.; Voorhees, P. M.; Berdeja, J. G.; Richardson, P. G.; Libby, E. N.; Wallace, E. E.; Birrer, N. E.; Burke, J. N.; Tamang, D. L.; Yang, M.; Jones, S. S.; Wheeler, C. A.; Markelewicz, R. J.; Raje, N. S. *Lancet Oncol*. **2016**, *17*, 1569-78.

[20] Li, Z. Y.; Zhang, C.; Zhang, Y.; Chen, L.; Chen, B. D.; Li, Q. Z.; Zhang, X. J.; Li, W. P. *Cancer Lett*. **2017**, *391*, 89-99.

[21] Weber, A.; Casini, A.; Heine, A.; Kuhn, D.; Supuran, C. T.; Scozzafava, A.; Klebe, G. *J. Med. Chem.* **2004**, *47*, 550-7.

[22] Alamdarsaravia, M.; Ghajarb, A.; Noorbalaa, AA.; Arbabia, M.; Emamic, A.; Shaheic, F.; Mirzaniac, M.; Jafariniaa, M.; Afaridehb, M.; Akhondzadeh, S. *Psychiatry Res*. **2017**, *255*, 59-65.

[23] Feng, T. T.; Wang, H.; Su, H.; Yu, L. Q.; Zhang, X. J.; Sun, H. P.; You, Q. D. *Bioorg. Med. Chem*. **2013**, *21*, 5339-54.

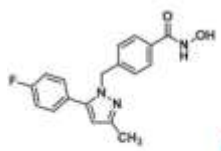

11i

IC_{50} (HDAC6) = 0.02 μM

IC_{50} (HDAC1) = 2.02 μM

GI_{50} (HpeG2) = 3.63 μM